

Photolysis of a caged peptide reveals rapid action of *N*-ethylmaleimide sensitive factor before neurotransmitter release

T. Kuner^{*†}, Y. Li^{**}, K. R. Gee[§], L. F. Bonewald[¶], and G. J. Augustine^{**†}

^{*}Department of Neurobiology, Duke University Medical Center, Box 3209, Durham, NC 27710; ^{**}Marine Biological Laboratory, Woods Hole, MA 02543; [§]Molecular Probes Invitrogen, Eugene, OR 97402; and [¶]School of Dentistry, University of Missouri, Kansas City, MO 64108-2784

Edited by Richard W. Tsien, Stanford University School of Medicine, Stanford, CA, and approved November 21, 2007 (received for review August 1, 2007)

The time at which the *N*-ethylmaleimide-sensitive factor (NSF) acts during synaptic vesicle (SV) trafficking was identified by time-controlled perturbation of NSF function with a photoactivatable inhibitory peptide. Photolysis of this caged peptide in the squid giant presynaptic terminal caused an abrupt (0.2 s) slowing of the kinetics of the postsynaptic current (PSC) and a more gradual (2–3 s) reduction in PSC amplitude. Based on the rapid rate of these inhibitory effects relative to the speed of SV recycling, we conclude that NSF functions in reactions that immediately precede neurotransmitter release. Our results indicate the locus of SNARE protein recycling in presynaptic terminals and reveal NSF as a potential target for rapid regulation of transmitter release.

caged probes | exocytosis | synaptic transmission | synaptic vesicle cycle

Neurotransmitter release relies on the precisely coordinated actions of many proteins that serve to recruit synaptic vesicles (SVs) to active zones, prepare SVs for Ca²⁺-dependent exocytosis, and recycle used components (1–5). At the core of these trafficking reactions lies the SNARE [soluble *N*-ethylmaleimide sensitive factor (NSF) attachment protein receptor] complex, which consists of proteins present in SVs (v-SNAREs) and the plasma membrane (t-SNAREs) (6). It is thought that *trans*-SNARE complexes bridging the SV and plasma membranes bring these two membranes into close apposition and mediate membrane fusion (7, 8). Because SNARE complexes are highly stable, hydrolysis of ATP by the molecular chaperone NSF (9, 10) is required to disassemble used SNARE complexes and, thereby, recycle SNARE proteins in preparation for future rounds of exocytosis (11–13). Although it is generally agreed that this action of NSF is important for neurotransmitter release, it is not clear whether NSF works before or after vesicle fusion. This distinction is critical for understanding the dynamic control of synaptic transmission by NSF and elucidating the life cycle of SNARE complexes during SV trafficking.

Two models have been proposed for the timing of NSF action during neurotransmitter release (Fig. 1). SNAREs could be disassembled just before fusion, meaning that NSF is active only when needed for a fusion reaction (Fig. 1*A*). This model is consistent with observations that NSF is required before vesicle fusion in several experimental systems (14–20). Alternatively, NSF could dissociate SNARE complexes immediately after neurotransmitter release (Fig. 1*B*). Such a postfusion action of NSF could provide an attractive mechanism for sorting of v- and t-SNAREs after fusion: in this case, newly separated v-SNAREs would be carried along as recycled SVs bud from the plasma membrane, whereas t-SNAREs would remain behind in the plasma membrane. Although experimental evidence supporting this conclusion is limited (21, 22), the ability to explain SNARE sorting makes a postfusion action of NSF part of most current models of SV trafficking (8, 23–26).

One way to distinguish between these two alternatives is to inactivate the function of NSF acutely in living presynaptic nerve terminals. A postfusion block of NSF would slowly inhibit

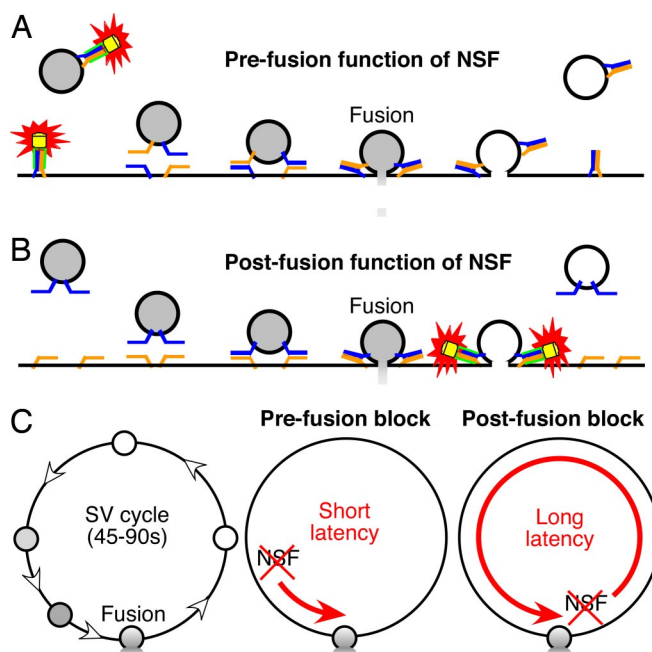


Fig. 1. Models of NSF function. (*A*) NSF acting upstream of neurotransmitter release. Colors indicate NSF (yellow), α SNAP (green), v-SNARE (blue), and t-SNAREs (orange). (*B*) Model showing a postfusion role of NSF. (*C*) Because the SV cycle requires 45–90 s (*Left*), a pre-fusion block of NSF action would occur much more quickly (*Center*), whereas a postfusion block would require all or most of the 45–90 s (*Right*).

transmitter release, over the 45–90 s required for SV cycling (27), whereas a pre-fusion block would more rapidly inhibit release (Fig. 1*C*). We therefore designed and synthesized a light-sensitive (caged) inhibitor of NSF. Our strategy was based on incorporating a caging group onto a key amino acid of a peptide that blocks the α SNAP-stimulated ATPase activity of NSF *in vitro* (28–30). This peptide prevents the NSF-mediated disassembly of the SNARE complex (30) and inhibits neurotransmitter release when injected into presynaptic terminals (28, 31).

Author contributions: T.K. and G.J.A. designed research; T.K. and Y.L. performed research; K.R.G. and L.F.B. contributed new reagents/analytic tools; T.K. and Y.L. analyzed data; and T.K. and G.J.A. wrote the paper.

The authors declare no conflict of interest.

This article is a PNAS Direct Submission.

[†]To whom correspondence should be sent at present address: Department of Anatomy and Cell Biology, University of Heidelberg, Im Neuenheimer Feld 307, 69120 Heidelberg, Germany. E-mail: kuner@uni-heidelberg.de.

This article contains supporting information online at www.pnas.org/cgi/content/full/0707197105/DC1.

© 2008 by The National Academy of Sciences of the USA

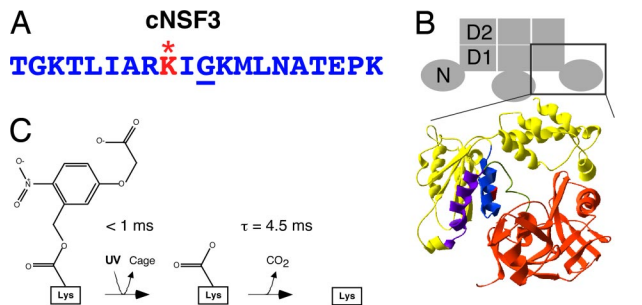


Fig. 2. Design of the cNSF3 peptide. (A) Sequence of the squid NSF3 peptide. Underlined residue is G309, the Comatose locus (corresponds to G274 in NSF-1 of *Drosophila*). The caged lysine residue K307 is in red and marked by *. (B) Schematic representation of NSF with structural elements contributing to the lateral surfaces of the N and D1 domains. (Upper) N, D1, and D2 denote the three domains of a NSF monomer; the schematic side view shows only three subunits of the hexamer. (Lower) Predicted structure of the N and D1 domains of NSF, based on coordinates taken from the NSF homologue P97 (71). The 2.5-nm-thick slab shows the N domain in orange, D1 domain in yellow, the NSF3 peptide in blue, and the caged lysine residue in red. Other active NSF peptides (28) are indicated in green (NSF1) and purple (NSF2). (C) Photochemistry of CMNCBZ-caged lysine. Absorption of a photon of UV light rapidly removes most of the cage, whereas a slower spontaneous decarboxylation removes the rest and generates free CO₂ (34).

By using this caged peptide to perturb NSF function, we found that the amount of neurotransmitter release was inhibited with a latency ranging from 1.6 to 3.2 s. Furthermore, the kinetics of neurotransmitter release was decreased even more rapidly, with a latency of 0.2 s. These very rapid actions of the uncaged inhibitory peptide lead us to conclude that the physiologically relevant locus of NSF action in the SV cycle is immediately upstream of membrane fusion and release of neurotransmitter.

Results

Design of Caged NSF3 (cNSF3) Peptide. Our caged NSF inhibitor was based on the NSF3 peptide (28) derived from the D1 domain of squid NSF (Fig. 2*A* and *B*). Structural data suggests that the amino acid residues constituting this peptide are located at the external surface of the D1 domain, in close proximity to the N domain (Fig. 2*B*, blue). A glycine residue within this segment of NSF (Fig. 2*A*, underlined) is critical for the actions of both NSF (32, 33) and the NSF3 peptide (28). We sought to disrupt the active conformation of the peptide by placing a caging group onto the side chain of an amino acid near this glycine. For this purpose, we used a ((5-carboxy-methoxy-2-nitrobenzyl)oxy)carbonyl (CMNCBZ) cage (Fig. 2*C*) that was attached to a surface-exposed lysine residue (Fig. 2*A*, red) two residues upstream of the critical glycine residue. After UV illumination, photolysis of this cage proceeds in two steps (Fig. 2*C*). The first step takes <1 ms and causes most of the cage to dissociate from the peptide; the second step, a spontaneous decarboxylation, is almost complete within 15 ms (34). The photolyzed peptide may assume its active conformation after the first step, but after the subsequent decarboxylation step it should be identical to the noncaged NSF3 peptide. Therefore the peptide should be in an active conformation within a few milliseconds or less after UV illumination.

Photolysis of Caged Peptide Inhibits Neurotransmitter Release. To define when NSF is required in the SV cycle, the cNSF3 peptide was microinjected into the presynaptic terminal of the squid giant synapse at concentrations of 0.05–2.5 mM, while we monitored synaptic transmission via recordings of presynaptic potentials and postsynaptic potentials (PSPs). The CMNCBZ cage masked the inhibitory activity of the peptide, because in each of 66 experiments uncaging the peptide with a brief pulse

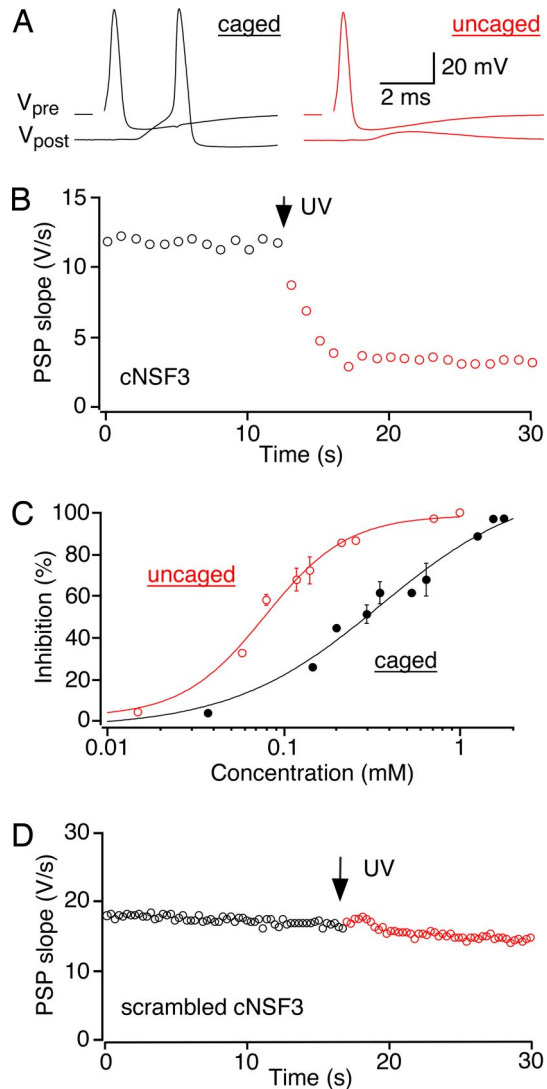


Fig. 3. Photolysis of cNSF in the presynaptic terminal. (A) Inhibition of synaptic transmission after uncaging microinjected cNSF3 (0.75 mM) in the giant terminal of the squid. Action potentials were elicited every 1 s. Simultaneous presynaptic (V_{pre}) and postsynaptic (V_{post}) voltage recordings immediately before (black) and after (red) uncaging (stimulation artifact blanked) are shown. (B) Rapid time course of inhibitory effects of uncaged NSF3. The slope of the PSP was determined from fits to the initial rise of the PSP and plotted as a function of time. UV light was applied for 50 ms (arrow, ≈ 150 mJ/mm²). The terminal was injected with 0.75 mM cNSF3. (C) Concentration-dependent inhibition of synaptic transmission by cNSF3 peptide (black closed circles, $n = 14$) and uncaged peptide (red open circles, $n = 14$). See *SI Text* for further details. (D) Lack of effect of photolysis of scrambled cNSF3 peptide (0.64 mM). UV light (750 mJ/mm²) was applied three times at the point indicated by the arrow.

of UV light inhibited synaptic transmission (Fig. 3*A*). The time course of this block was rapid, occurring within a few seconds or less (Fig. 3*B*). Synaptic transmission decreased during cNSF3 injection, indicating that the cage did not completely neutralize peptide activity (Fig. 3*C*). However, the CMNCBZ cage caused a 4-fold increase in the IC₅₀ of cNSF3 (0.35 ± 0.08 mM) compared with noncaged peptide (0.08 ± 0.01 mM), which gave us sufficient dynamic range to control NSF function.

Previous work has established the specificity of noncaged NSF3 peptide. Key arguments are that: (i) both NSF3 and another peptide from the external surface of the D1 domain have identical inhibitory effects on both ATPase activity and synaptic

transmission; and (ii) mutation of the glycine residue, which inhibits NSF function *in vivo* (32, 33), completely abolishes the ability of NSF3 to inhibit both ATPase activity and synaptic transmission (28). Mass spectroscopy reveals that exposure to UV light produces a peptide that is identical to uncaged NSF3 (unpublished data), so that the biochemical properties of NSF3 defined in previous work (28, 31) should fully apply to uncaged cNSF3. Nonetheless, to consider possible side effects of uncaging cNSF3, we performed two control experiments. First, we uncaged a scrambled NSF3 peptide. This peptide had the same amino acid composition as cNSF3, including the presence of a CMNCBZ-caged lysine residue, but it does not resemble NSF3. In a total of 11 experiments, photolysis of this control peptide produced no effect on synaptic transmission, even when illuminating the terminal with up to 750 mJ/mm² and at free cage concentrations as high as 0.9 mM (Fig. 3D). Photolysis of a second control compound, CMNCBZ-caged rhodamine, was similarly ineffective ($n = 5$; data not shown). These results indicate that inhibition of neurotransmitter release was caused directly by the liberated NSF3 peptide, rather than by UV illumination or production of free CMNCBZ cage or CO₂. Thus, caging a single lysine residue decreased the biological activity of the NSF3 peptide ≈ 4 -fold, allowing flash photolysis to very rapidly control the molecular machinery of neurotransmitter release.

The NSF3 peptide both decreases synaptic transmission and slows the kinetics of neurotransmitter release (28). To determine the relationship between these two actions, we examined how quickly each developed after cNSF3 photolysis. For this purpose, postsynaptic currents (PSCs) were recorded while photolyzing cNSF3. Fig. 4A shows a series of simultaneous presynaptic and postsynaptic recordings during photolysis of cNSF3. PSCs were elicited every second, with the preflash PSC shown as a black trace in Fig. 4A. After a pulse of UV light, which was applied at the same time as a presynaptic action potential, the next PSC was virtually unchanged in amplitude, yet clearly had slower kinetics (Fig. 4A, largest red trace). Both PSC rise time and decay were slowed after peptide uncaging, as readily observed when comparing PSCs scaled with the same peak amplitude (Fig. 4B). Although this change in PSC kinetics was virtually immediate, occurring in <1 s, the inhibition of PSC amplitude required several seconds for completion (Fig. 4C). Similar results were obtained in a total of 14 experiments. Hence, temporally precise activation of the caged peptide revealed distinct time courses for the two actions of NSF3: a fast effect on the kinetics of neurotransmitter release and a slower effect on the amount of neurotransmitter released.

Time Course of the Two Responses to Uncaged NSF3. We quantified the time course of the slow effect of NSF3 by fitting exponential functions to data such as those shown in Fig. 4C *Upper*. The time constant for inhibiting PSC amplitude was activity-dependent and ranged from 3.1 s at 0.2 Hz to 1.6 s at 5 Hz (Fig. 5A). This acceleration of the rate of inhibition at higher rates of stimulation is consistent with previous observations of the activity dependence of this peptide (28) and full-length NSF (32, 33). Uncaged NSF3 also had some effect in the absence of activity: when stimulating at 0.2 Hz, the first PSC evoked 5 s after photolysis of the peptide was reduced by 75% (Fig. 5A). This finding may reflect a continuous activity of NSF (20) in the resting presynaptic terminal. Thus, NSF regulates the amount of neurotransmitter release over a time scale of a few seconds or less.

Given the rapid effect of uncaged NSF3 upon release kinetics, a different procedure was needed to determine the time course of this effect. For this purpose, we uncaged cNSF3 at different intervals preceding an action potential (Fig. 5B *Inset*). At very brief time intervals, the amount of slowing of PSC kinetics was minimal, but the slowing effect was complete if the light flash

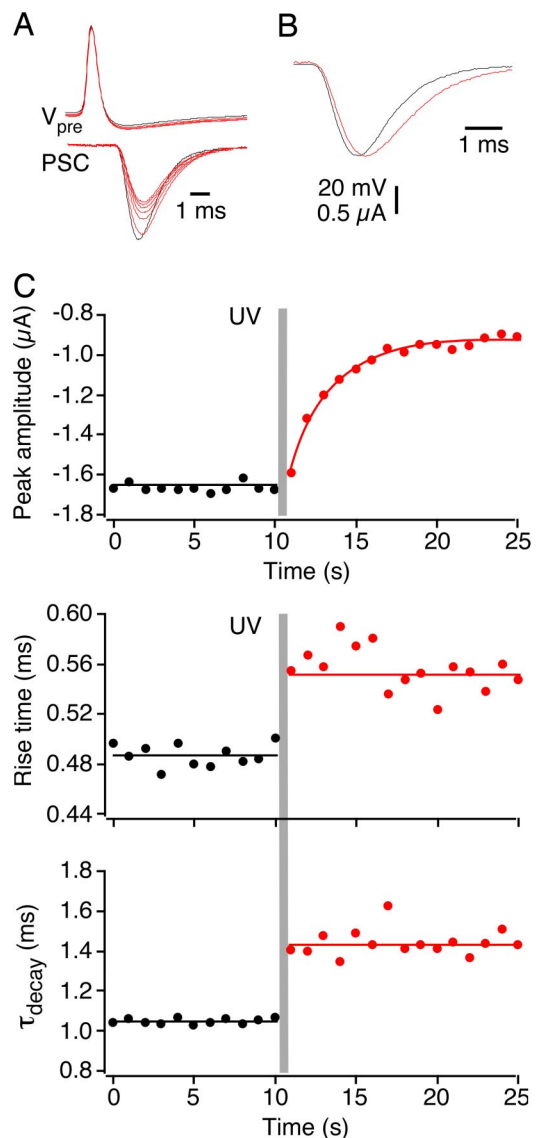


Fig. 4. Differential onset of amplitude and kinetic effect. (A) Simultaneous presynaptic and postsynaptic recordings before (black line) and after (red line) photolysis of cNSF3 peptide. Synapse was stimulated at 1 Hz. (B) Scaled PSCs, from the experiment shown in A, before (black) and after (red) uncaging of NSF3. (C) Onset of changes in PSC amplitude (Top), PSC rise time (20–80%; Middle), and PSC decay time constant (Bottom). UV light (150 mJ/mm²) was applied at the 10-s time point (gray bar).

occurred 1 s before the synapse was activated. The relationship between preflash interval (Δt) and degree of slowing of the PSC decay was described by an exponential function with a time constant of 0.22 s (Fig. 5B). This time constant represents an upper estimate of the time period when NSF3 affects release kinetics, because of possible delays associated with photolysis of the CMNCBZ cage and with binding of uncaged NSF3 peptide to its target. Therefore, NSF regulates the kinetics of release over a time scale of 0.22 s or faster.

Because the time scales of the inhibitory effects of uncaged NSF3 peptide are very rapid relative to the tens of seconds or longer required for vesicles to recycle via conventional [45–90 s (27)] or kiss-and-run [$t \approx 20$ s (35, 36)] mechanisms of endocytosis, our data argue that NSF is required before neurotransmitter release occurs rather than acting after membrane fusion (Fig. 1). However, the rate of synaptic activity in the experiments

provide a temporal benchmark for future studies of the timing of other exocytotic interactions.

Materials and Methods

Caged Peptides. CMNCBZ-caged lysine (67, 68) was synthesized as described in [\[supporting information \(SI\) Text\]](#). This peptide was used to synthesize the following peptides: cNSF3, TGKTLIAR[K]IGKMLNATEPK (squid sequence) and scrambled cNSF3, GNIELATK[K]ARIKLTPMKG. Details of peptide synthesis are provided in [SI Text](#).

Electrophysiology. The stellate ganglion was dissected from *Loligo pealei*, and recordings of synaptic transmission were done as described (69, 70). Caged

peptide was microinjected into the giant presynaptic terminal and a shuttered argon ion laser (Coherent) was used for peptide photolysis. More details are described in [SI Text](#).

ACKNOWLEDGMENTS. We thank H. Tokumaru for many discussions and help with biochemical experiments; T. Schweizer for technical assistance; J. Rizo for suggesting NMR interaction studies of the NSF3 peptide with NSF domains; F. Filipp and M. Sattler for performing NMR interaction studies; and P. Hanson for discussions. T.K. was supported by a Grass Fellowship in Neuroscience, an Human Frontier Science Program long-term fellowship, and the Feodor-Lynen Program of the Alexander von Humboldt Foundation. Y.L. received a American Heart Association predoctoral fellowship. The research also was supported by National Institutes of Health Grants NS-21624 and NS-1771.

1. Augustine GJ, Burns ME, DeBello WM, Hilfiker S, Morgan JR, Schweizer FE, Tokumaru H, Umayahara K (1999) *J Physiol (London)* 520:33–41.
2. Rettig J, Neher E (2002) *Science* 298:781–785.
3. Jahn R, Südhof TC (1999) *Annu Rev Biochem* 68:863–911.
4. Südhof TC (1995) *Nature* 375:645–653.
5. Rothman JE (1994) *Nature* 372:55–63.
6. Sollner T, Whiteheart SW, Brunner M, Erdjument BH, Geromanos S, Tempst P, Rothman JE (1993) *Nature* 362:318–324.
7. Weber T, Zemelman BV, McNew JA, Westermann B, Gmachl M, Parlati F, Sollner TH, Rothman JE (1998) *Cell* 92:759–772.
8. Jahn R, Lang T, Südhof TC (2003) *Cell* 112:519–533.
9. Block MR, Glick BS, Wilcox CA, Wieland FT, Rothman JE (1988) *Proc Natl Acad Sci USA* 85:7852–7856.
10. Wilson DW, Wilcox CA, Flynn GC, Chen E, Kuang WJ, Henzel WJ, Block MR, Ullrich A, Rothman JE (1989) *Nature* 339:355–359.
11. Sollner T, Bennett MK, Whiteheart SW, Scheller RH, Rothman JE (1993) *Cell* 75:409–418.
12. Hanson PI, Roth R, Morisaki H, Jahn R, Heuser JE (1997) *Cell* 90:523–535.
13. Zinsmaier KE, Bronk P (2001) *Biochem Pharmacol* 62:1–11.
14. Banerjee A, Barry VA, DasGupta BR, Martin T (1996) *J Biol Chem* 271:20223–226.
15. Burgoyne RD, Williams G (1997) *FEBS Lett* 414:349–352.
16. Colombo MI, Taddese M, Whiteheart SW, Stahl PD (1996) *J Biol Chem* 271:18810–18816.
17. Mayer A, Wickner W, Haas A (1996) *Cell* 85:83–94.
18. Nichols BJ, Ungermann C, Pelham HR, Wickner WT, Haas A (1997) *Nature* 387:199–202.
19. Tolar LA, Pallanck L (1998) *J Neurosci* 18:10250–10256.
20. Xu T, Ashery U, Burgoyne RD, Neher E (1999) *EMBO J* 18:3293–3304.
21. Grote E, Carr CM, Novick PJ (2000) *J Cell Biol* 151:439–452.
22. Littleton JT, Barnard RJ, Titus SA, Slind J, Chapman ER, Ganetzky B (2001) *Proc Natl Acad Sci USA* 98:12233–12238.
23. Chen YA, Scheller RH (2001) *Nat Rev Mol Cell Biol* 2:98–106.
24. Li L, Chin, LS (2003) *Cell Mol Life Sci* 60:942–960.
25. Richmond JE, Broadie KS (2002) *Curr Opin Neurobiol* 12:499–507.
26. Rizo J, Südhof TC (2002) *Nat Rev Neurosci* 3:641–653.
27. Betz WJ, Wu LG (1995) *Curr Biol* 5:1098–1101.
28. Schweizer FE, Dresbach T, DeBello WM, O'Connor V, Augustine GJ, Betz H (1998) *Science* 279:1203–1206.
29. Polgar J, Reed GL (1999) *Blood* 94:1313–1318.
30. Matsushita K, Morrell CN, Cambien B, Yang SX, Yamakuchi M, Bao C, Hara MR, Quick RA, Cao W, O'Rourke B, et al. (2003) *Cell* 115:139–150.
31. Parnas I, Rashkovan G, O'Connor V, El-Far O, Betz H, Parnas H (2006) *J Neurophysiol* 96:1053–1060.
32. Kawasaki F, Mattiuz AM, Ordway RW (1998) *J Neurosci* 18:10241–10249.
33. Littleton JT, Chapman ER, Kreber R, Garment MB, Carlson SD, Ganetzky B (1998) *Neuron* 21:401–413.
34. Papageorgiou G, Corrie JET (1997) *Tetrahedron* 53:3917–3932.
35. Aravanis AM, Pyle JT, Tsien RW (2003) *Nature* 423:643–647.
36. Gandhi SP, Stevens CF (2003) *Nature* 423:607–613.
37. Brunger AT, DeLaBarre B (2003) *FEBS Lett* 555:126–133.
38. Malhotra V, Orci L, Glick BS, Block MR, Rothman JE (1988) *Cell* 54:221–227.
39. Orci L, Malhotra V, Amherdt M, Serafini T, Rothman JE (1989) *Cell* 56:357–368.
40. Murthy VN, Stevens CF (1999) *Nat Neurosci* 2:503–507.
41. Hong RM, Mori H, Fukui T, Moriyama Y, Futai M, Yamamoto A, Tashiro Y, Tagaya M (1994) *FEBS Lett* 350:253–257.
42. Klenchin VA, Martin TFJ (2000) *Biochimie* 82:399–407.
43. Otto H, Hanson PI, Jahn R (1997) *Proc Natl Acad Sci USA* 94:6197–6201.
44. Steel GJ, Tagaya M, Woodman PG (1996) *EMBO J* 15:745–752.
45. Taubenblatt P, Dedieu JC, Gulik-Krzywicki T, Morel N (1999) *J Cell Sci* 112:3359–3367.
46. Ungermann C, Sato K, Wickner W (1998) *Nature* 396:543–548.
47. Walch-Solimena C, Blasi J, Edelmann L, Chapman ER, von Mollard GF, Jahn R (1995) *J Cell Biol* 128:637–645.
48. Fernandez-Alfonso T, Kwan R, Ryan TA (2006) *Neuron* 51:179–186.
49. Lang T, Margittai M, Holzler H, Jahn R (2002) *J Cell Biol* 158:751–760.
50. Takamori S, Holt M, Stenius K, Lemke EA, Grønborg M, Riedel D, Urlaub H, Schenck S, Brügger B, Ringler P, et al. (2006) *Cell* 127:831–846.
51. Fasshauer D, Otto H, Eliason WK, Jahn R, Brunger AT (1997) *J Biol Chem* 272:28036–28041.
52. An SJ, Almers W (2004) *Science* 306:1042–1046.
53. Matveeva E, Whiteheart SW (1998) *FEBS Lett* 435:211–214.
54. Hatsuzawa K, Lang T, Fasshauer D, Bruns D, Jahn R (2003) *J Biol Chem* 278:31159–31166.
55. Peters C, Baars TL, Buhler S, Mayer A (2004) *Cell* 119:667–678.
56. Müller JM, Rabouille C, Newman R, Shorter J, Freemont P, Schiavo G, Warren G, Shima DT (1999) *Nat Cell Biol* 1:335–340.
57. Otter-Nilsson M, Hendriks R, Pecheur-Huet EI, Hoekstra D, Nilsson T (1999) *EMBO J* 18:2074–2083.
58. Müller O, Bayer MJ, Peters C, Andersen JS, Mann M, Mayer A (2002) *EMBO J* 21:259–269.
59. Zenisek D, Steyer JA, Almers W (2000) *Nature* 406:849–854.
60. Holz RW, Bittner MA, Peppers SC, Senter RA, Eberhard DA (1989) *J Biol Chem* 264:5412–5419.
61. Parsons TD, Coorsen JR, Horstmann H, Almers W (1995) *Neuron* 15:1085–1096.
62. Tagaya M, Wilson DW, Brunner M, Arango N, Rothman JE (1993) *J Biol Chem* 268:2662–2666.
63. Tokumaru H, Umayahara K, Pellegrini LL, Ishizuka T, Saisu H, Betz H, Augustine GJ, Abe T (2001) *Cell* 104:421–432.
64. Liu Y, Cheng K, Gong K, Fu AK, Ip NY (2006) *J Biol Chem* 281:9852–9858.
65. Matveeva EA, Whiteheart SW, Vanaman TC, Slevin JT (2001) *J Biol Chem* 276:12174–12181.
66. Huynh H, Bottini N, Williams S, Cherepanov V, Musumeci L, Saito K, Bruckner S, Vachon E, Wang X, Kruger J, et al. (2004) *Nat Cell Biol* 6:831–839.
67. Mitchison TJ, Sawin KE, Theriot JA, Gee K, Mallavarapu A (1998) *Methods Enzymol* 291:63–78.
68. Gee KR, Weinberg ES, Kozlowski DJ (2001) *Bioorg Med Chem Lett* 11:2181–2183.
69. Augustine GJ, Eckert R (1984) *J Physiol (London)* 346:257–271.
70. Augustine GJ, Charlton MP, Smith SJ (1985) *J Physiol (London)* 367:143–162.
71. Zhang X, Shaw A, Bates P, Newman R, Gowen B, Orlova E, Gorman M, Kondo H, Dokurno P, Lally J, et al. (2000) *Mol Cell* 6:1473–1484.